Mössbauer study of local electronic and magnetic properties of Pt-substituted Fe-Ni Invar

2000 J. Phys.: Condens. Matter 12 2079

(http://iopscience.iop.org/0953-8984/12/9/312)

J. Phys.: Condens. Matter **12** (2000) 2079–2091. Printed in the UK PII: S0953-8984(00)05665-4

Mössbauer study of local electronic and magnetic properties of Pt-substituted Fe–Ni Invar

Y Kong†‖, F S Li†, M Kaack‡, J Pelzl‡, P Stauche§ and H Bach§

† Department of Physics & The Applied Magnetics Laboratory of the Ministry of Education, Lanzhou University, 730000 Lanzhou, People's Republic of China
‡ Institut für Experimentalphysik III, Fakultät für Physik und Astronomie, Ruhr-Universität Bochum, 44780 Bochum, Germany
§ Institut für Experimentalphysik IV, Fakultät für Physik und Astronomie, Ruhr-Universität Bochum, 44780 Bochum, Germany

Received 5 July 1999, in final form 5 January 2000

Abstract. The Mössbauer effect in $Fe_{65}Ni_{35-x}Pt_x$ ($x = 0$, 5.6 and 10.8) has been measured at temperatures between 4.2 K and 300 K to study local electronic and magnetic properties of the system. The variation of the hyperfine-field distribution with temperature has confirmed the transitions of Fe atoms from a high-magnetic-moment (HM) state to a low-magnetic-moment (LM) state with elevating temperature and a simple model based on a two-state transition interpreted well the changes of the hyperfine-field distribution with Pt content and temperature. The substitution of Pt for Ni makes the HM $\rightarrow$ LM transition of Fe atoms more difficult and decreases the chemical disorder in the sample. By using the composition dependence of the lattice volume, the volume effect and the pure substitution effect of the Pt atom on the average hyperfine field were further separated. Moreover, the Debye temperatures of the samples were evaluated from the decrease of the isomer shift with increasing temperature.

1. Introduction

Since the early finding [1] by Guillaume the Invar effect has been observed in many different kinds of material and more and more physical anomalies have to be considered as Invar-typical (for reviews, see references [2–4]). In spite of extensive experimental and theoretical efforts, the origin of the Invar effect has never been fully understood. It has been however accepted that strong moment–volume coupling and a complex thermal-excitation process as well as negative lattice anharmonicity distinguish an Invar system from a normal metal or alloy. On the basis of experimental findings [5–7] and theoretical predictions [8–11], the moment–volume instability (MVI) has been considered as a critical feature of materials that exhibit the Invar effect.

The fcc FeNi alloy with Fe concentration around 65 at.% and the FePt alloy containing around 75 at.% iron are two classical Invar systems. While there are many similarities, remarkable differences in properties between the two systems have been reported [3, 12, 13]. For example, on approach to the γ–α phase boundary, the magnetic moment $m(x)$ of Fe–Ni Invar obviously deviates from the Slater–Pauling curve, and this is accompanied by a decrease in T_C, but no such a deviation occurs in Fe–Pt Invar; in some Invar-related physical properties [3, 12], FeNi Invar exhibits magnetic softening when compared to the magnetically

‖ Present address: Max-Planck Institut für Festkörperforschung, Heisenbergstrasse 1, D-70569 Stuttgart, Germany.

0953-8984/00/092079+13$30.00

'hard' FePt alloys; furthermore, a stronger magnetovolume effect [13] in FePt Invar than in FeNi alloys is observed.

In order to obtain a better understanding of the Invar effect, it is both necessary and very interesting to investigate the reason for the differences between the two Invar systems. With Pt substituting for Ni, FeNiPt [14, 15] systems form a 'bridge' connecting Fe–Ni with Fe–Pt systems, and one can continuously study the changes of Invar-related properties from FeNi to FePt Invar. This may lead to the mechanism that led to the difference in properties between the two systems becoming well understood. On the other hand, the lattice volume of FeNi alloy is expanded by the substitution of Pt for Ni, and thus we should expect to observe the MVI; the magnetovolume effect in the FeNiPt system can therefore be investigated.

In the present work, ^{57}Fe Mössbauer spectroscopy has been applied to study the local electronic and magnetic properties of Pt-substituted $Fe_{65}Ni_{35}$. As an effective microprobe for detecting the local properties of Mössbauer nuclei in material, Mössbauer spectroscopy has been extensively applied to Invar materials [16–19]. In a series of works [20–22] Abd-Elmeguid *et al* have systematically investigated the moment–volume coupling in Invar alloys. From measurements of the high-pressure Mössbauer effect, they have obtained experimental evidence for HM $\rightarrow$ LM transitions in Fe–Ni and Fe–Pt Invar. To the authors' knowledge, however, no results have been reported to date for ternary FeNiPt Invar systems in the literature.

By measuring the Mössbauer effect in $Fe_{65}Ni_{35-x}Pt_x$ ($x = 0$, 5.6 and 10.8) and its temperature dependence, in the present study, we have investigated the variations of the hyperfine parameters with composition (Pt content) and temperature in the framework of the MVI and discussed the substitution effect of Pt atoms in detail.

It should be mentioned that in the present work the Mössbauer measurements were performed on powder samples that were filed from single-crystal $Fe_{65}Ni_{35-x}Pt_x$, which have been used to study the elastic anomalies [23] in the system. In view of the fact that the magnetic anisotropy of FeNi(Pt) Invar [24] is rather small, the use of single-crystal powder in Mössbauer measurements should be irrelevant as regards discussing the results obtained.

2. Experimental details

Single crystals of $Fe_{65}Ni_{35-x}Pt_x$ ($x = 0$, 5.6, 10.8) were grown by a modified Bridgman–Stockbarger technique. The details of the growth and characterization of the single crystals have been given elsewhere [23]. The compositions of the crystals, $Fe_{63.4}Ni_{36.6}$, $Fe_{63.9}Ni_{30.5}Pt_{5.6}$ and $Fe_{64.0}Ni_{25.2}Pt_{10.8}$, were determined by microprobe SEM with energy-dispersive analysis of the characteristic x-ray. Within the accuracy of 1 at.%, no deviations from homogeneity were observed. X-ray diffraction investigations with Cu Kα radiation were carried out on powders filed from single crystals. From the diffraction patterns shown in figure 1, we see that all three samples have the characteristic disordered fcc lattice and no other phase is indicated, although there is a little broadening of the peaks due to the stresses induced by the filing process. The lattice constants were estimated to be 3.593 Å, 3.626 Å and 3.656 Å for $x = 0$, 5.6 and 10.8 respectively.

For some of the fine powders filed from the crystals of $Fe_{65}Ni_{35-x}Pt_x$, ^{57}Fe transmission Mössbauer spectra were collected using a constant-acceleration conventional spectrometer with a liquid-helium cryostat at selected temperatures between 4.2 K and 300 K. The γ-ray source was ^{57}Co in a Rh matrix. The maximal drive velocity is calibrated by measuring the spectrum of a 25 μm thin foil of α-Fe.

Since the $Fe_{65}Ni_{35-x}Pt_x$ Invar samples investigated are chemically disordered, the spectra of the samples all manifest distribution of the hyperfine parameters and thus must be analysed with a distribution-fitting procedure. In this study, two different distribution-fitting methods,

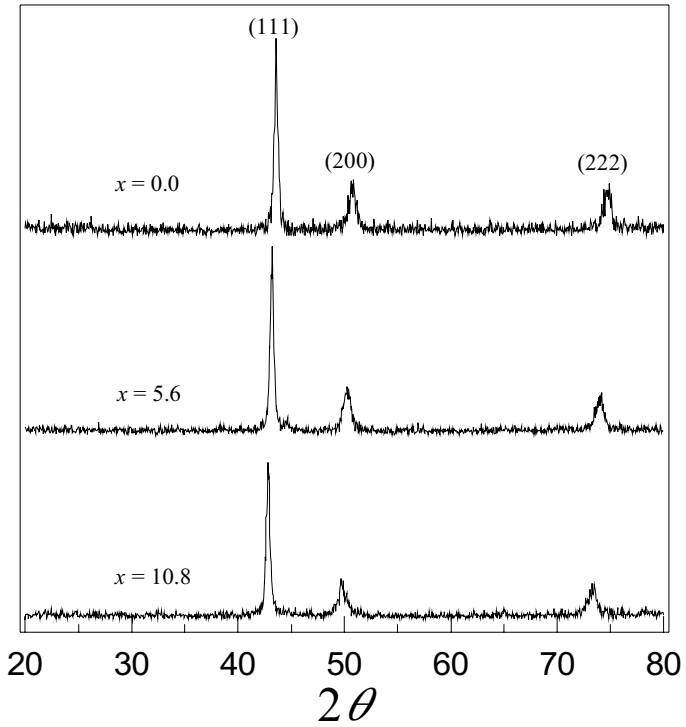

Figure 1. X-ray diffraction patterns of $Fe_{65}Ni_{35-x}Pt_x$ powders ($x = 0$, 5.6 and 10.8) filed from single crystals.

which are based on the Voigt-function method [25,26] and the Hesse–Rübartsch technique [27], are applied to obtain reliable hyperfine-field distributions (HFDs) $P(B_{eff})$. For all of the spectra measured, the HFDs $P(B_{eff})$ obtained by the two fitting procedures proved to be nearly the same. In the following, only the results obtained by the Voigt-function method are presented.

3. Results and discussion

3.1. The Mössbauer effect and its temperature dependence

The Mössbauer spectra of $Fe_{65}Ni_{35-x}Pt_x$ with $x = 0$ and $x = 10.8$ obtained at various temperatures are respectively shown in figure 2 and figure 3. All the spectra exhibit ferromagnetic sextet splitting. Compared to those for $x = 10.8$, the spectra for $x = 0$ show obvious sagging from the baseline. The observation that the relative intensities of the third and fourth peaks in the spectra are extraordinarily large and increase with temperature leads us to suggest that the spectra contain certain subspectra with rather lower hyperfine fields, and that the proportions of those components increase with temperature.

The weighted-average hyperfine parameters of the spectra at 4.2 and 300 K are listed in table 1, where the average effective hyperfine field $\overline{B_{eff}}$ is defined by

$$\overline{B_{eff}} = \left(\int B_{eff} P(B_{eff})\, \mathrm{d}B_{eff}\right) \Big/ \left(\int P(B_{eff})\, \mathrm{d}B_{eff}\right) \tag{1}$$

where $P(B_{eff})$ is the probability of the distribution. The substitution of Pt for Ni increases

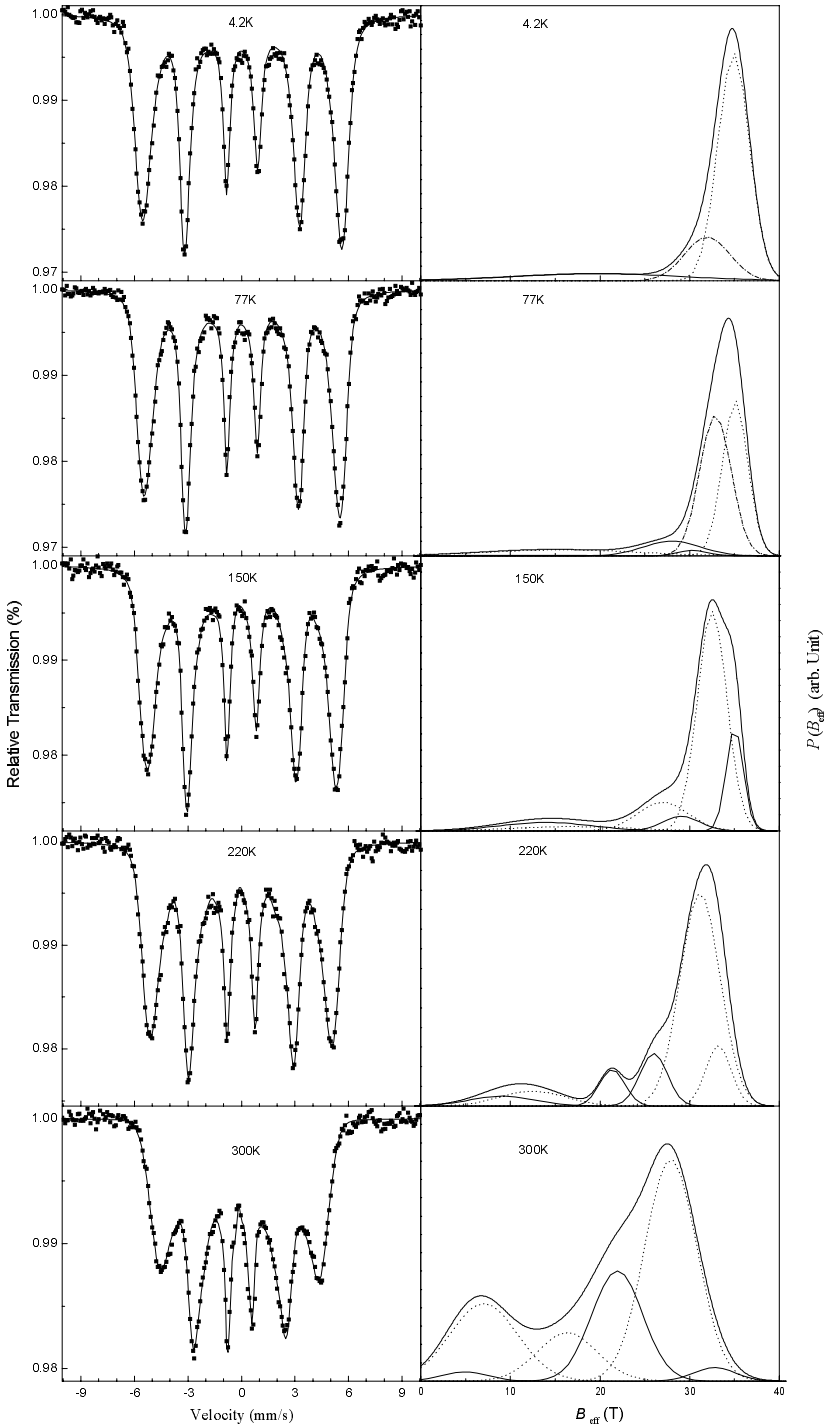

Figure 2. The Mössbauer effect in $Fe_{65}Ni_{35-x}Pt_x$ with $x = 0$ at various temperatures and the corresponding hyperfine-field distributions. The fine and dashed lines are the fitted Gaussians.

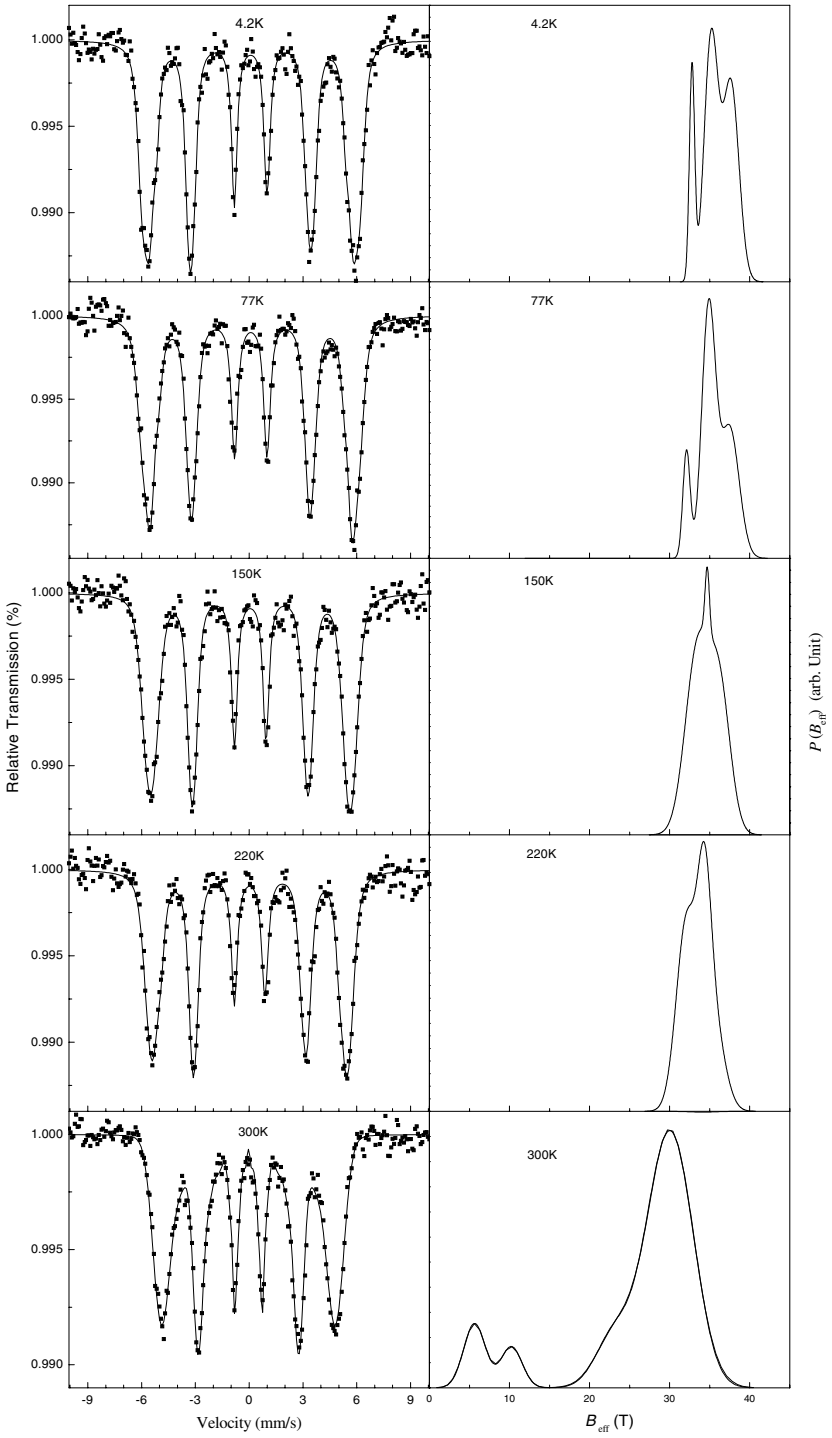

Figure 3. The Mössbauer effect in $Fe_{65}Ni_{35-x}Pt_x$ with $x = 10.8$ at various temperatures and the corresponding hyperfine-field distributions.

Table 1. Average hyperfine parameters of $Fe_{65}Ni_{35-x}Pt_x$ with $x = 0$ and $x = 10.8$ at 4.2 K and 300 K. $\overline{B_{eff}}$: average hyperfine field in teslas; $\overline{\delta}$: average isomer shift in mm s^{-1}; $\overline{Q_s}$: average quadruple splitting in mm s^{-1}.

	4.2 K			300 K		
	$\overline{B_{eff}}$	$\overline{\delta}$	$\overline{Q_s}$	$\overline{B_{eff}}$	$\overline{\delta}$	$\overline{Q_s}$
$x = 0$	32.6 ± 0.1	0.05 ± 0.04	0.04 ± 0.04	20.9 ± 0.1	-0.09 ± 0.04	0.03 ± 0.04
$x = 10.8$	35.8 ± 0.1	0.09 ± 0.04	0.01 ± 0.04	26.0 ± 0.1	-0.04 ± 0.04	0.00 ± 0.04

$\overline{B_{eff}}$ and the average isomer shift $\overline{\delta}$, compared to the results listed for $x = 0$, but decreases the average quadruple splitting $\overline{Q_s}$. All three parameters decrease with increasing temperature.

The variations of $\overline{B_{eff}}$ and $\overline{\delta}$ with temperature are shown in figures 4(a) and 4(b), respectively. The decrease of $\overline{B_{eff}}$ with the increase of the measuring temperature indicates different characters for $x = 0$ and $x = 10.8$. While below 220 K $\overline{B_{eff}}$ for $x = 0$ manifests a larger reduction than that for $x = 10.8$, which indicates magnetic softening in Fe–Ni Invar,

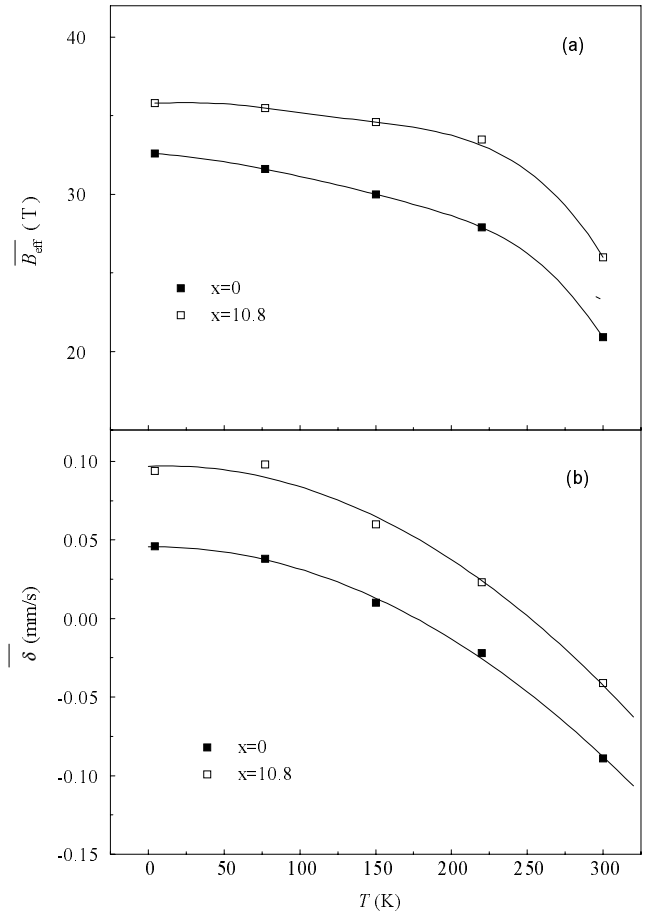

Figure 4. Temperature dependences of (a) the average effective hyperfine field and (b) the average isomer shift of $Fe_{65}Ni_{35-x}Pt_x$ with $x = 0$ and $x = 10.8$.

$\overline{B_{eff}}$ for $x = 10.8$ decreases at a higher rate on increasing the temperature further. Previous investigations on the spontaneous magnetization M_s of Invar alloys [3] have suggested that the temperature behaviour of M_s is affected by not only the conventional spin-wave excitation but also a 'hidden' second excitation. In view of the close relationship of $\overline{B_{eff}}$ with the Fe magnetic moment, it could be argued that the reduction of $\overline{B_{eff}}$ with temperature is also caused by both spin-wave and 'hidden' second excitations. On the basis of the MVI in the Invar system and the considerable low-field components observed in the Mössbauer spectra with increasing temperature, the HM $\rightarrow$ LM transition of Fe atoms with elevating temperature may be reasonably considered as a 'hidden' excitation. The different temperature behaviours of the $\overline{B_{eff}}$ observed for $x = 0$ and $x = 10.8$ could therefore be attributed to different HM $\rightarrow$ LM transitions in the two samples.

The average isomer shifts $\overline{\delta}$ of $Fe_{65}Ni_{35-x}Pt_x$ with $x = 0$ and $x = 10.8$ show large reductions with increasing temperature, too. It is well known that the isomer shift is the sum of the chemical isomer shift δ_0 and the contribution from the second-order Doppler shift δ_{SOD}, i.e.

$$\delta = \delta_0 + \delta_{SOD}. \tag{2}$$

In general, the first term of the above expression is temperature independent, but the Doppler shift is directly related to the lattice dynamics of the sample. If $\langle v^2 \rangle$ is the mean square velocity of the Mössbauer atom in the lattice, δ_{SOD} can be expressed as

$$\delta_{SOD} = -\frac{\langle v^2 \rangle}{2c}. \tag{3}$$

Within the Debye model of the lattice dynamics, the Debye temperature Θ_D of the sample can be evaluated by fitting the experimental δ to the following equation:

$$\delta(T_1) - \delta(T_2) = \frac{9k}{2Mc}\left[T_2\left(\frac{T_2}{\Theta_D}\right)^3 \int_0^{\Theta_D/T_2} \frac{x^3}{e^x - 1}\,dx - T_1\left(\frac{T_1}{\Theta_D}\right)^3 \int_0^{\Theta_D/T_1} \frac{x^3}{e^x - 1}\,dx\right] \tag{4}$$

where k is the Boltzmann constant, M is the mass of the Mössbauer nucleus and T_2 is the lowest temperature. Using the minimum-standard-deviation method, the average isomer shifts $\overline{\delta}$ of $Fe_{65}Ni_{35-x}Pt_x$ were fitted to the above equation. The fitted results which are plotted as lines in figure 4(b) give values of $\Theta_D = 385$ K for $x = 0$ and 300 K for $x = 10.8$. The value of Θ_D obtained for $x = 0$ is larger than the value 348 K [28] derived from the low-temperature specific heat but agrees well with the result 400 K [29] obtained by extrapolating the temperature dependence of the elastic constants.

3.2. Hyperfine-field distribution

As mentioned above, the Mössbauer spectra of $Fe_{65}Ni_{35-x}Pt_x$ are not well resolved due to the chemical disorder in the samples. Hyperfine parameters (especially the hyperfine fields) of ^{57}Fe atoms with different local environments do not show discrete components but form a broad distribution.

The resulting HFDs for $Fe_{65}Ni_{35-x}Pt_x$ at 300 K are shown in figure 5. It is noticed that the broad peak at high fields around 30 T dominates the HFDs of the samples, but for all three samples there are, to some extent, low-field components in their HFDs extending to about 0 T. In particular, a non-zero probability at $B_{eff} = 0$ T for $x = 0$ is observed. With increasing x, the distribution width of the probability peaks in the HFDs tends to become smaller and the low-field peaks in the HFD for $x = 0$ change into two well-resolved narrower peaks. In the meantime, the hyperfine-field components in the intermediate-field range from 10 T to 25 T decrease with increasing x.

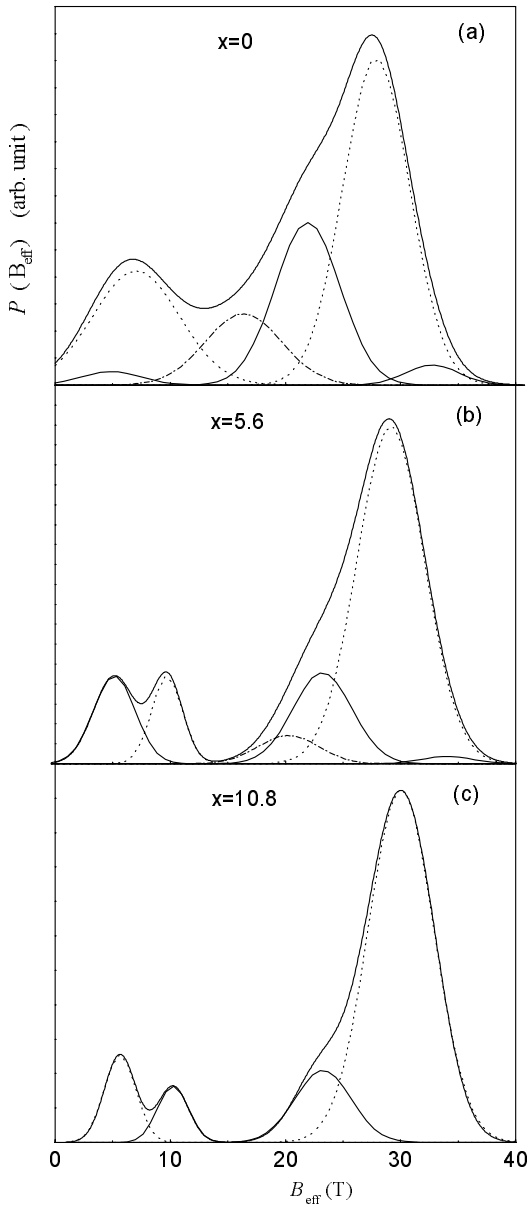

Figure 5. Hyperfine-field distributions in $Fe_{65}Ni_{35-x}Pt_x$ at 300 K. The fine and dashed lines are the fitted Gaussians.

A simple Weiss-like two-state model based on the MVI may be adopted to interpret the HFDs in $Fe_{65}Ni_{35-x}Pt_x$ at 300 K. For simplicity, the two magnetic states of the atoms are assumed to be the HM state with the usual local magnetic moment and the LM state with zero magnetic moment and higher energy than the HM state. With increasing temperature, the higher-energy LM states are gradually occupied with a certain population fraction. By neglecting the details of the interactions between the ^{57}Fe Mössbauer nucleus and its n_i neighbours and considering a unique hyperfine coupling constant $D = D_{ij}$, the effective

hyperfine field of the Fe atom with the ith local environment can be written as [30, 31]

$$B_{eff}(i) = A_{\mathrm{Fe}}\mu_{\mathrm{Fe}}(i) + n_i D\overline{\mu} \tag{5}$$

where the small contribution $A_s\mu_s$ of the local conduction electron spin polarization has been omitted. Here the first term is the contribution of the on-site local magnetic moment but the latter arises from neighbouring magnetic atoms and is described as a transferred hyperfine field. Depending on the details of the interactions between the atoms, D may be positive or negative. But for transition metal or alloy the transferred field usually gives a contribution, which partially counteracts the contribution of the local magnetic moment. For the $Fe_{65}Ni_{35-x}Pt_x$ investigated, at 300 K, some atoms are in the LM state and others remain in the HM state. By taking into account the contribution from nearest neighbours (NN), B_{eff} for a HM Fe atom with a total of twelve NN, among which n atoms are in the LM state, is given by

$$B_{eff}^{HM} = A_{\mathrm{Fe}}\mu_{\mathrm{Fe}} + D(12-n)\overline{\mu} \tag{6}$$

and B_{eff} for a LM Fe atom with n LM nearest neighbours is given by

$$B_{eff}^{LM} = D(12-n)\overline{\mu}. \tag{7}$$

With the addition of next-nearest-neighbouring contributions, B_{eff} for such an Fe atom will build a Gaussian-type distribution around B_{eff}^{HM} (B_{eff}^{LM}) with a certain width w. Then, B_{eff} for the sample is described by the distribution [16]

$$P(B_{eff}) = (1-\alpha)\sum_n P(n)\exp\left(-\frac{[B_{eff} - B_{eff}^{HM}(n)]^2}{w^2}\right) + \alpha\sum_n P(n)\exp\left(-\frac{[B_{eff} - B_{eff}^{LM}(n)]^2}{w^2}\right) \tag{8}$$

where $P(n)$ is the probability of finding an Fe atom with n LM nearest neighbours and α the population fraction of the LM states at the measurement temperature. Because of the diversity of local environments of Fe atoms in samples, different B_{eff}^{HM} and B_{eff}^{LM} may cause $P(B_{eff})$ to spread over the range from high field to low field; this is just like the observation for the HFDs shown in figure 5.

Independent Gaussians with different positions and widths have been used to fit the HFDs of $Fe_{65}Ni_{35-x}Pt_x$ at 300 K. The results are shown in figure 5 by fine or dashed lines and the positions and widths obtained are listed in table 2. As indicated by the table, the HFDs of $Fe_{65}Ni_{35-x}Pt_x$ with $x = 0$, 5.6 and 10.8 could be well reproduced by using six, six and four Gaussians, respectively. It is indicated that at 300 K the atom distribution in $Fe_{65}Ni_{35-x}Pt_x$ and the transition from HM to LM states build many Fe local environments, among which only six, six and four Fe environments are dominantly populated for the cases of $x = 0$, 5.6 and 10.8. From expressions (6) and (7), a qualitative prediction as regards these local environments of Fe atoms may be made as follows: the high-field components ($\geqslant$25 T) come from the HM Fe atoms with more LM neighbours, the intermediate-field components (10 T $\leqslant B_0 \leqslant$ 25 T) are mostly contributed by the HM Fe atoms with more HM neighbours and the low-field components ($\leqslant$10 T) result from by those LM atoms that have different HM neighbours. With increasing x, the centres of the Gaussians shift towards the high-field side. According to (6) and (7), the shifting of the Gaussian centre should be attributed to a larger average and local Fe magnetic moment. It is indirectly indicated that the substitution of Pt for Ni raises the magnetic moments of the atoms. On the other hand, a smaller relative area of the low-field Gaussians ($B_0 \leqslant$ 10 T) was observed with increasing Pt content and should be related to there being fewer LM atoms in the samples with larger x. It is suggested that the substitution of Pt for Ni makes the transition of the Fe atoms from HM to LM states more difficult. With increasing

Table 2. Positions B_0, widths w and relative areas S of the independent Gaussians fitted to the HFDs of $Fe_{65}Ni_{35-x}Pt_x$ at 300 K.

Sample	No of Gaussians	S (in %)	B_0 (in T)	w (in T)
$x = 0$	1	1.6 ± 0.5	4.9 ± 0.1	5.2 ± 0.1
	2	19.9 ± 0.5	7.0 ± 0.1	7.5 ± 0.1
	3	11.0 ± 0.5	16.4 ± 0.1	6.6 ± 0.1
	4	21.3 ± 0.5	21.9 ± 0.1	5.7 ± 0.1
	5	44.0 ± 0.5	27.9 ± 0.1	5.8 ± 0.1
	6	2.2 ± 0.5	32.8 ± 0.1	4.6 ± 0.1
$x = 5.6$	1	10.0 ± 0.5	5.1 ± 0.1	3.6 ± 0.1
	2	7.5 ± 0.5	9.7 ± 0.1	2.7 ± 0.1
	3	4.7 ± 0.5	20.2 ± 0.1	5.3 ± 0.1
	4	14.7 ± 0.5	23.3 ± 0.1	5.1 ± 0.1
	5	62.1 ± 0.5	29.2 ± 0.1	5.8 ± 0.1
	6	1.0 ± 0.5	34.1 ± 0.1	4.4 ± 0.1
$x = 10.8$	1	8.7 ± 0.5	5.6 ± 0.1	2.7 ± 0.1
	2	5.3 ± 0.5	10.2 ± 0.1	2.7 ± 0.1
	3	—	—	—
	4	12.7 ± 0.5	23.3 ± 0.1	4.9 ± 0.1
	5	73.3 ± 0.5	30.0 ± 0.1	5.7 ± 0.1
	6	—	—	—

Pt content, additionally, it was observed that the third and sixth Gaussians tend to disappear. Taking this in combination with the narrower HFD with increasing x and the Gaussian peaks becoming more discrete, it could be argued that the substitution of Pt for Ni decreases the chemical disorder in $Fe_{65}Ni_{35}$.

The HFDs obtained for the Mössbauer spectra of $Fe_{65}Ni_{35-x}Pt_x$ with $x = 0$ at various temperatures have already been plotted in figure 2. At low temperature, 4.2 K, the HFD for $x = 0$ forms a well-defined but broadened Gaussian peak at high fields of about 35 T. The broadening of the peak may be caused by the difference in the local environment of the Fe atom, which is produced by the chemical disorder of the atom distribution. With increasing temperature above 77 K, an obvious probability on the low-field side has been observed, which indicates that some Fe atoms are already in LM states. In a sense, a temperature around 77 K seems to be a critical temperature for the HM $\rightarrow$ LM transition of atoms in $Fe_{65}Ni_{35-x}Pt_x$ with $x = 0$. On increasing the temperature further, more low-field components arise, corresponding to more LM atoms existing in the sample. Furthermore, the HFDs, shown in figure 2, have also been fitted using independent Gaussians with various positions and widths and the results are plotted in the same figure. The fitted results for 77 K, 150 K and 220 K are listed in table 3. Combined with the results at 300 K listed in table 2, the change of relative areas S of the individual Gaussians distinctly indicates a temperature variation of the population fraction of Fe atoms with different local environments, which should be attributed to the relative change of the fractions of Fe atoms in HM and LM states.

Figure 3 also shows the HFDs for selected Mössbauer spectra of $Fe_{65}Ni_{35-x}Pt_x$ with $x = 10.8$ at various temperatures. The low-temperature HFDs show well-defined discrete three-peak structures, which indicates three dominant local environments of Fe atoms in the sample. It is confirmed that the substitution of Pt for Ni decreases the chemical disorder in FeNi Invar compared with those for $x = 0$ shown in figure 2. By neglecting the population of the LM states at low temperature, qualitatively, the peak centred at smaller hyperfine field should

Table 3. Fitted Gaussians for the HFDs of $Fe_{65}Ni_{35-x}Pt_x$ with $x = 0$ at 77 K, 150 K and 220 K. Here B_0, w and S are the positions, the widths and the relative areas of the independent Gaussians.

Temperature	No of Gaussians	S (in %)	B_0 (in T)	w (in T)
77 K	1	0.6 ± 0.5	11.3 ± 0.1	10.9 ± 0.1
	2	8.8 ± 0.5	15.8 ± 0.1	17.0 ± 0.1
	3	8.1 ± 0.5	28.0 ± 0.1	6.3 ± 0.1
	4	1.6 ± 0.5	30.4 ± 0.1	3.3 ± 0.1
	5	42.7 ± 0.5	32.9 ± 0.1	3.5 ± 0.1
	6	38.2 ± 0.5	35.1 ± 0.1	2.8 ± 0.1
150 K	1	6.8 ± 0.5	13.9 ± 0.1	10.3 ± 0.1
	2	4.6 ± 0.5	16.8 ± 0.1	13.6 ± 0.1
	3	12.6 ± 0.5	27.0 ± 0.1	5.7 ± 0.1
	4	4.7 ± 0.5	29.0 ± 0.1	4.2 ± 0.1
	5	56.0 ± 0.5	32.5 ± 0.1	3.3 ± 0.1
	6	15.3 ± 0.5	35.0 ± 0.1	1.9 ± 0.1
220 K	1	4.6 ± 0.5	9.1 ± 0.1	7.4 ± 0.1
	2	7.0 ± 0.5	12.5 ± 0.1	7.4 ± 0.1
	3	6.6 ± 0.5	21.4 ± 0.1	2.8 ± 0.1
	4	10.3 ± 0.5	26.0 ± 0.1	3.1 ± 0.1
	5	60.6 ± 0.5	31.2 ± 0.1	4.5 ± 0.1
	6	10.9 ± 0.5	33.2 ± 0.1	2.8 ± 0.1

be attributed to the Fe atoms with more Fe neighbours. Up to 220 K, no finite probability on the low-field side of the HFD is found and a higher critical temperature for the HM $\rightarrow$ LM transition of atoms in $Fe_{65}Ni_{35-x}Pt_x$ with $x = 10.8$ may thus be supposed. This is consistent with the results of the theoretical investigation [32] of the electronic structure of FeNi and FePt Invar, from which it has been concluded that the energy difference between HM and LM states in FePt Invar is larger than that in FeNi Invar.

3.3. The substitution effect of Pt

As observed from table 1, the substitution of Pt for Ni raises $\overline{B_{eff}}$ for Fe atoms due to the enlarged average magnetic moment $\overline{\mu}$ in $Fe_{65}Ni_{35-x}Pt_x$. At 4.2 K, the increase of $\overline{B_{eff}}$ can be evaluated to be $\mathrm{d}\ln\overline{B_{eff}}/\mathrm{d}x \approx 9 \times 10^{-3}$, which is a little smaller than that of $\overline{\mu}$, $\mathrm{d}\ln\overline{\mu}/\mathrm{d}x \approx 11 \times 10^{-3}$, derived from the measured average magnetic moment [33].

The increase of $\overline{B_{eff}}$ in $Fe_{65}Ni_{35-x}Pt_x$ with increasing Pt content can be divided into two contributions: one comes from the volume expansion produced by volume-larger Pt atoms and another is the pure substitution effect, which is in fact caused by the Pt-induced change in the interactions between the atoms. Thus the variation of $\overline{B_{eff}}$ with Pt content may be written as

$$\frac{\mathrm{d}\ln\overline{B_{eff}}}{\mathrm{d}x} = \left(\frac{\partial\ln\overline{B_{eff}}}{\partial x}\right)_{V,T} + \left(\frac{\partial\ln\overline{B_{eff}}}{\partial V}\right)_{x,T}\left(\frac{\partial V}{\partial x}\right)_{T} \tag{9}$$

where $\mathrm{d}\ln\overline{B_{eff}}/\mathrm{d}x$ is the change of $\overline{B_{eff}}$ with x obtained from measured Mössbauer spectra. The first term on the right-hand side denotes the pure substitution effect and the second term

$$\left(\frac{\partial\ln\overline{B_{eff}}}{\partial V}\right)_{x,T}\left(\frac{\partial V}{\partial x}\right)_{T} = -\frac{B}{V}\left(\frac{\partial\ln\overline{B_{eff}}}{\partial p}\right)_{x,T}\left(\frac{\partial V}{\partial x}\right)_{T} \tag{10}$$

with bulk modulus B is just the effect of the volume expansion.

By using the pressure dependence [20] $\partial \ln \overline{B_{eff}}/\partial p = -4.4 \times 10^{-2}$ GPa^{-1} of $\overline{B_{eff}}$ for $Fe_{65}Ni_{35}$ at 4.2 K together with the observed bulk modulus $B = 219.2$ GPa† for $x = 0$ and the lattice constants a of $Fe_{65}Ni_{35-x}Pt_x$, the contribution of the volume expansion to the increase of $\overline{B_{eff}}$ at 4.2 K can be evaluated from equation (10) and then the contribution of the pure substitution effect can be derived from (9). The observed increase of $\overline{B_{eff}}$ at 4.2 K and the two derived contributions are listed in table 4. It is noticed that the effect of the volume expansion caused by the Pt atoms raises the average effective hyperfine field but, in contrast, the pure substitution effect of substituting Pt for Ni produces the opposite effect of reducing the average hyperfine field. This is consistent with our conclusions based on theoretical investigations on iron–nickel nitrides [34], in which the substitution of Ni for Fe changes the interactions between Fe and its neighbours and decreases the average Fe magnetic moment, contrasting with the positive $(\partial \ln \overline{\mu}/\partial V)_x$. As a final consequence, the larger volume effect of Pt increases $\overline{B_{eff}}$ for $Fe_{65}Ni_{35-x}Pt_x$ after compensating for the negative contribution of the pure substitution effect.

Table 4. Variations of $\overline{B_{eff}}$ and $\overline{\mu}$ for $Fe_{65}Ni_{35-x}Pt_x$ at 4.2 K with x and separate contributions. Here the symbol A denotes $\overline{B_{eff}}$ and $\overline{\mu}$. For the physical meaning of the individual contributions, see the text.

A	$\mathrm{d} \ln A/\mathrm{d}x$	$(\partial \ln A/\partial x)_{V,T}$	$(\partial \ln A/\partial V)_{x,T}(\partial V/\partial x)_T$
$\overline{B_{eff}}$	$(9 \pm 0.1) \times 10^{-3}$	$(-3.9 \pm 0.1) \times 10^{-2}$	$(4.8 \pm 0.1) \times 10^{-2}$
$\overline{\mu}$	$(11.0 \pm 0.1) \times 10^{-3}$	$(-4.0 \pm 0.1) \times 10^{-2}$	$(5.1 \pm 0.1) \times 10^{-2}$

To examine the difference between the changes of the hyperfine field and the magnetic moment, in a similar way, the variation of $\overline{\mu}$ [33] with x can also be decomposed into contributions from the volume expansion and from the pure substitution effect by using the experimental value [12] $\mathrm{d} \ln M_s/\mathrm{d}p = -4.7 \times 10^{-2}$ GPa^{-1} of the pressure dependence of the spontaneous magnetization obtained for $Fe_{65}Ni_{35}$ at 4.2 K and under $p \approx 2$ GPa. The results are also listed in table 4. Note that here $\mathrm{d} \ln M_s/\mathrm{d}p \approx \mathrm{d} \ln \overline{\mu}/\mathrm{d}p$ is assumed. The near equality of the variations of $\overline{B_{eff}}$ and $\overline{\mu}$ with x and that of their decomposed contributions suggest that the variation of $\overline{B_{eff}}$ is dominated by the local spin structure.

4. Conclusions

From the measurements of the Mössbauer effect at selected temperatures up to 300 K, the hyperfine interactions in $Fe_{65}Ni_{35-x}Pt_x$ ($x = 0$, 5.6 and 10.8) and its composition and temperature dependences have been investigated for the first time.

The variation of the average hyperfine magnetic field with temperature confirmed the transitions of the Fe atoms from HM to LM states with elevating temperature. A Weiss-like two-state model was applied to explain the change in hyperfine-field distribution with composition and temperature. It was concluded that the substitution of Pt for Ni makes the HM $\rightarrow$ LM transition more difficult by raising the energy difference between the two states. On the other hand, the substitution of Pt for Ni decreases the chemical disorder of the atom distribution in the sample. The contributions of the volume effect and the pure substitution effect of Pt atoms to the room-temperature average effective hyperfine field have been separated out and compared with the contributions of the two effects to the average magnetic moment. From the variation of the isomer shift with temperature, the Debye temperature of $Fe_{65}Ni_{35-x}Pt_x$ was estimated to be 385 K for $x = 0$ and 300 K for $x = 10.8$.

† A value extrapolated from high temperature without the low-temperature anomaly; see [23].

Acknowledgments

One of the authors (Y Kong) wishes to express his thanks to DAAD (Deutscher Akademischer Austauschdienst) for the financial support of his study/research stay in Germany. The authors are greatly indebted to Professor Dr A H Morrish, Dr Rongjie Zhou, Dr Xuezhi Zhou and Mr Zhengwen Li in Manitoba, Canada, for their help with the measurements of Mössbauer spectra. This work was partially supported by the National Science Foundation of China.

References

[1] Guillaume Ch E 1897 *C. R. Acad. Sci., Paris* **125** 235
[2] Wassermann E F 1989 *Phys. Scr.* T **25** 209
[3] Wassermann E F 1990 *Ferromagnetic Materials* vol 5, ed K H J Buschow and E P Wohlfarth (Amsterdam: North-Holland) p 240
[4] Wassermann E F 1991 *J. Magn. Magn. Mater.* **100** 346
[5] Nicholson D M, Chowdhary A and Schwartz L 1984 *Phys. Rev.* B **29** 1633
[6] Kisker E, Wasserman E F and Carbone C 1987 *Phys. Rev. Lett.* **58** 1784
[7] James R D and Kinderlehrer D 1994 *J. Appl. Phys.* **75** 7012
[8] Moruzzi V L 1989 *Physica* B **161** 99
[9] Entel P, Hoffmann E, Mohn P, Schwarz K and Moruzzi V L 1993 *Phys. Rev.* B **47** 8706
[10] Abrikosov I A, Eriksson O, Söderlind P, Skriver H L and Johansson B 1995 *Phys. Rev.* B **51** 1058
[11] Hayn R and Drchal V 1998 *Phys. Rev.* B **58** 4341
[12] Hayashi K and Möri N 1981 *Solid State Commun.* **38** 1057
[13] Sumiyama K, Shiga M, Morioka M and Nakamura Y 1979 *J. Phys. F: Met. Phys.* **9** 1665
[14] Kußmann A and Jensen K 1958 *Arch. Eisenhüttenwesen* **29** 585
[15] Rellinghaus B 1995 Thermische Anregungen und Magnetovolumen Effekte in $Fe_{72}Pt_{28}$ und $Fe_{65}Ni_{35-x}Pt_x$ *Thesis* Duisburg University
[16] Shiga M and Nakamura Y 1984 *J. Magn. Magn. Mater.* **40** 319
[17] Ullrich H and Hesse J 1984 *J. Magn. Magn. Mater.* **45** 315
[18] Abd-Elmeguid M M, Hobuss U, Micklitz H, Huck B and Hesse J 1987 *Phys. Rev.* B **35** 4796
[19] Bandyopadhyay D 1999 *J. Phys.: Condens. Matter* **11** 1199
[20] Abd-Elmeguid M M, Schleede B and Micklitz H 1988 *J. Magn. Magn. Mater.* **72** 253
[21] Abd-Elmeguid M M and Micklitz H 1989 *Phys. Rev.* B **40** 7395
[22] Abd-Elmeguid M M and Micklitz H 1989 *Physica* B **161** 17
[23] Kong Y, Kaack M, Pelzl J, Li F S, Stauche P and Bach H 2000 unpublished
[24] Kagawa H and Chikazumi S 1980 *J. Phys. Soc. Japan* **48** 1476
[25] Rancourt D G and Ping J Y 1991 *Nucl. Instrum. Methods Phys. Res.* B **58** 85
[26] Ping J Y, Rancourt D G and Dunlap R A 1992 *J. Magn. Magn. Mater.* **103** 285
[27] Hesse J and Rübartsch A 1974 *J. Phys. E: Sci. Instrum.* **7** 526
[28] Caudron C, Meunier J and Costa P 1974 *Solid State Commun.* **14** 975
[29] Tanji Y 1971 *J. Phys. Soc. Japan* **31** 1366
[30] Akai H, Akai M, Blügel S, Drittler B, Ebert H, Terakura D, Zeller R and Dederichs P H 1990 *Prog. Theor. Phys. Suppl.* **101** 11
[31] Zhang Y D, Budnick J I, Ford J C and Hines W A 1991 *J. Magn. Magn. Mater.* **100** 13
[32] Entel P and Schröter M 1989 *Physica* B **161** 160
[33] Kong Y 1999 *PhD Thesis* Lanzhou University (in English)
[34] Kong Y and Li F S 1998 *Phys. Rev.* B **57** 970